Biochemical Pharmacology, Vol. 32, No. 24, pp. 3679–3694, 1983.
Printed in Great Britain.

0006-2952/83 $3.00 + 0.00

INTERACTIONS OF ACRIDINE ORANGE WITH NUCLEIC ACIDS

PROPERTIES OF COMPLEXES OF ACRIDINE ORANGE WITH SINGLE STRANDED RIBONUCLEIC ACID

JAN KAPUSCINSKI,* ZBIGNIEW DARZYNKIEWICZ and MYRON R. MELAMED
Memorial Sloan–Kettering Cancer Center, New York, NY 10021, U.S.A.

(*Received* 31 *January* 1983; *accepted* 14 *April* 1983)

Abstract—Interactions between acridine orange (AO) and nucleic acids (calf thymus DNA, and homoribo- and homodeoxyribo-polynucleotides) were studied in solutions containing ethanol as a cosolvent. Light absorption, scattering and luminescence were measured as a function of AO concentration at different dye/phosphate (D/P) ratios, and the data were analyzed using the McGhee–von Hippel probabilistic model of the polymer–ligand interactions. The absorption spectra of AO complexes with four homoribopolymers are presented. The intrinsic association constants and cooperativity coefficients of the formation of the complexes were calculated. The effects of ethanol (up to 35%, v/v) on these interactions were concentration dependent and may be extrapolated to zero concentration of this cosolvent. The possibility of destabilization of the double helix of nucleic acids by AO at high D/P ratios is discussed in light of the available thermodynamic data.

Interest in studying the interactions of acridine dyes with nucleic acids stems from the fact that these dyes exhibit a variety of important properties. Thus, they have antibacterial and mutagenic activities and their structures and modes of binding resemble other biologically active chemicals such as carcinogens, certain antibiotics or proteins [1]. In addition, some dyes, such as acridine orange (AO)†, show metachromasia (the color of the dye changes, usually toward the red, when bound to certain cellular components), a phenomenon which is responsible for its wide application for analytical purposes, especially in cytochemistry.

The metachromatic properties of AO in interactions with nucleic acids were the subject of extensive studies during the past four decades (for reviews see Refs. 2 and 3). While it is clear that the dye intercalates into double stranded (ds) nucleic acids, the mechanism of its binding to single stranded (ss) nucleic acids still remains unclear. The present interpretation of the metachromasia of AO upon binding to ss-nucleic acids assumes electrostatic interactions between the nucleic acids and the dye, and subsequent formation of dye-stacks along the nucleic acid backbone (for reviews see Refs. 3 and 4). This interpretation, however, fails to explain a variety of properties of the nucleic acid–AO complexes (e.g. Refs. 2, 3, 5 and 6).

Studies of the interaction of AO with biopolymers are hindered by several peculiarities of the dye. One is the propensity of the dye to form dimers and higher aggregates, resulting in a multicomponent spectrum that is difficult to analyze [7]. Also, the dye is adsorbed by various surfaces, including glass; this phenomenon decreases the accuracy of such techniques as dialysis or filtration. Finally, the complexes of AO with ss-nucleic acids are poorly soluble and precipitate during titrations [6]. The precipitation, often neglected in previous studies, may alter the spectral data and also be a source of inaccuracies in calculations based on the mass action law. In the present studies we have tried to circumvent the above obstacles by studying interactions of AO with synthetic RNA and DNA homopolymers and with calf thymus DNA in solutions containing ethanol. The influence of ethanol, as a cosolvent, on complex formation was studied separately. The results were analyzed using the theoretical model of McGhee and von Hippel [8] which, albeit originally developed for large ligand–polymer interactions, has been applied successfully to investigations of small intercalators and even of inorganic cations (e.g. Refs. 9–11).

* Address all correspondence to: Jan Kapuscinski, Ph.D., Memorial Sloan–Kettering Cancer Center, Walker Laboratory, 145 Boston Post Road, Rye, NY 10580.

† Abbreviations: AO; 3,6-bis(dimethylamino)acridine hydrochloride = acridine orange; ss; single stranded; ds, double stranded; D/P, dye/phosphate molar ratio; r, binding density; n, binding site size; ω, cooperativity coefficient; K, association constant; C_F and C_B, free and bound dye concentrations; E_λ, molar extinction coefficient; $\Delta G^0 = -RT\ln K$, Gibbs free energy change; and Hepes, 4-(2-hydroxyethyl)-1-piperazine-ethanesulfonic acid.

MATERIALS AND METHODS

Acridine orange. (AO), chromatographically purified, was obtained from Polysciences (Warrington, PA) and used without further purification. The stock solution of 1.58mM was made in distilled water. Dye concentrations were estimated colorimetrically at the isosbestic point of the monomer–dimer system, using

values of the molar absorption coefficients of $E_{470} = 4.33 \times 10^4\ M^{-1}\ cm^{-1}$ for aqueous solutions [12] and of $E_{473} = 4.76 \times 10^4\ M^{-1}\ cm^{-1}$ for solutions containing 25% (v/v) ethanol. Most measurements were made in a standard solution containing 10 mM Na_2HPO_4-NaH_2PO_4 and 1 mM EDTA at pH 7.0, in the presence (25%) or absence of ethanol. When other solvents were used, the value of E was adjusted accordingly.

Nucleic acids. RNA homopolymers poly(rA), poly(rC), poly(rI), and poly(rU), obtained from P-L Biochemicals, Inc. (Milwaukee, WI), were used without additional purification. Their concentrations (in 100 mM NaCl, 5 mM Hepes, 1 mM EDTA, pH 7.0) were estimated spectrophotometrically using molar absorption coefficients given by the vendor. Coefficient corrections were made when other solvents were used. Calf-thymus DNA (Type I, Sigma) concentration was determined as for the homoribopolymers. All other chemicals were of the highest commercial grade.

Spectrophotometric measurements. These measurements were carried out with a Zeiss PM6 spectrophotometer equipped with a temperature control unit (25 ± 0.05°). The spectra, in digital form, at 1 or 2 nm increments were transferred into a Hewlett–Packard (HP) 9815S computer, stored on magnetic tape, processed using an SLM PR-8000 spectrum-processing program, and drawn by an HP 7225A graphic plotter connected to the computer.

The measurements were carried out in quartz cuvettes with a light path of 1 cm or less, depending on dye concentration, to avoid absorption above 1.8. The cuvettes were prewashed three times with a small volume of the measured solution to minimize the effect of adsorption of the dye to the walls of the cuvettes.

Titrations of the nucleic acids with AO were performed in conical Sarstedt plastic test tubes [12], each containing 2 ml of RNA solution. The aliquots (1–100 μl) of AO stock solution were adeed to each tube. The mixtures were then thoroughly stirred, kept at 25° for 20 hr, centrifuged (~ 400 *g* for 10 min) and examined for the presence of a precipitate [6]; only samples with no visible precipitate were measured. The error resulting from the adsorption of AO to the test tube surfaces was estimated in each series of experiments (twice) by absorption measurements of an aliquot of the AO solution, prior to and after exposure to the test tube.

To obtain the association constant for binding density (r) < 0.3, the titrations were done directly in cuvettes. In these cases, the absorption increments at 474 and 494 nm were measured in two cuvettes, one containing nucleic acid and the other containing buffer alone. The measurements were made 10 min following addition of the aliquots of AO solution (1–5 μl). Measurements of cuvettes containing AO solution alone provided estimates of the extinction coefficient of the free dye in different solutions. Because the extinction coefficient of nucleic acids varied depending on the ethanol and salt concentrations, multiple titrations of nucleic acids in various solutions and in the standard buffer, for which the coefficient was known, were always carried out.

Fluorescence emission spectra. Spectra were measured with an SLM 4800 (Urbana, IL) spectrofluorimeter, equipped with a thermostatic cuvette chamber (25 ± 0.1°), a quartz cuvette (0.3 × 0.3 cm i.d.), and a 450W Xenon lamp, and interfaced to a computer and digital graphic plotter. The excitation wavelength was set at the isosbestic point (4 nm band width). The emission spectra (4 nm band width), recorded on magnetic tape, were processed using the SLM PR-8000 program. All results were corrected for the inner filter effect; this correction extended the linear concentration–fluorescence relationship up to an O.D. of 3.0 [6, 13].

Light scattering measurements. These measurements were done at right angle geometry, using the SLM-4800 spectrofluorimeter, with no polarizers. The excitation and emission monochromators were set at the same wavelength (350 nm). For titrations, a solution of nucleic acid of known concentration was placed in the square (1 cm) quartz cuvette equipped with a magnetic stirrer. The scattered light was measured at 10 min after the addition of aliquots of AO, using the ratio mode, with glycogen solution as a standard. The results are expressed as a ratio of the intensity of scattered light of the sample to the intensity of scatter of the nucleic acid solution alone. The effect of increase of free dye concentration has been found to be negligible.

RESULTS

The first experiments were directed towards selection of the optimal cosolvent, and analysis of the cosolvent effect on the physicochemical properties of the reactants and products.

Solubilities of AO–RNA complexes, at various D/P ratios (up to 2.0), were tested by adding aliquots of AO stock solution to 50 μM RNA dissolved in a mixture of the buffer and organic solvent and were inspected for the presence of precipitate following centrifugation 20 hr later [6]. Ethanol, dioxane, dimethylformamide and dimethyl sulfoxide at concentrations up to 50% (v/v) were tested. The best solubility was observed in solutions containing ethanol and dioxane; ethanol at a concentration of 25% (v/v) was then arbitrarily chosen for most experiments reported in this paper.

In the presence of 5–35% ethanol, increased optical density of homoribopolymers was observed, especially for poly(rA) and poly(rC). Thus, the extinction coefficients at 260 nm of poly(rA) and poly(rC) were increased by 20 and 27%, respectively, in the presence of 25% (v/v) ethanol.

The effect of ethanol on dsDNA was less pronounced. Extinction of dsDNA was increased by less than 10% in the presence of up to 35% ethanol.

Ethanol markedly decreased dimerization of AO. The constant of dimerization, measured as described by von Tscharner and Schwarz [12], was found to be $9.1 \times 10^3\ M^{-1}$ in aqueous buffer and $9.0 \times 10^4\ M^{-1}$ in buffer containing 25% ethanol. This large difference indicates that, at an AO concentration of 20 μM, for example, monomers are only 78% of the monomers–dimer total in aqueous solution but are over 96% in a solution of 25% ethanol.

Ethanol induced red shifts in the maximum of absorption and in the isosbestic point for the

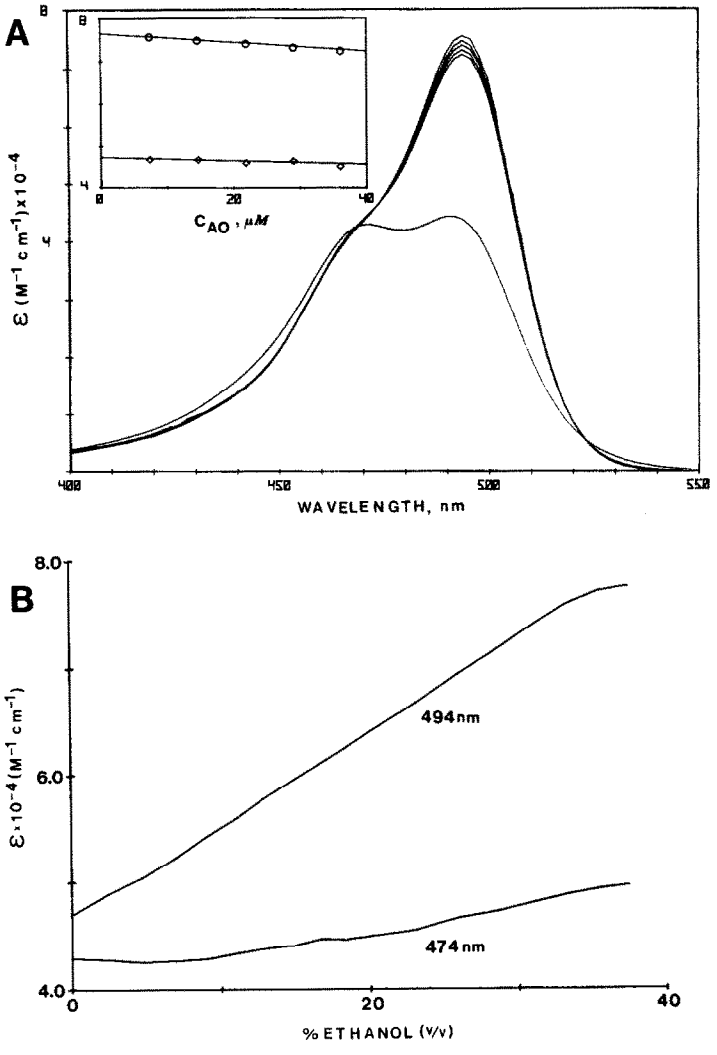

Fig. 1. (A) Absorption spectra of AO. From top to bottom AO concentrations: 7.5, 15, 22, 29, 36 and 40 μM. All samples were measured in standard buffer [25% (v/v) ethanol] except 40 μM which was measured in the absence of ethanol. Insert: Changes in the molar extinction coefficient at: (○) 494 and (◇) 474 nm (isosbestic point) as a function of AO concentration [standard buffer, 25% (v/v) ethanol]. (B) Change of molar extinction coefficient of AO at 494 nm and at 474 nm as a function of ethanol concentration (50 mM Na^+, 5 mM Hepes, pH 7.0).

monomer–dimer system (Fig. 1, Table 1) and a 2 nm blue shift in the maximum of AO emission.

Titration of calf thymus DNA with AO is shown in Fig. 2. The red shift of the maximum absorption and the hypochromic effect, both characteristic of dye interaction, are not much different in the presence or absence of ethanol [14]. The presence of a well defined isosbestic point (Fig. 2, insert) shows lack of precipitation of the complex during titration. By extrapolation of the reciprocal of the hyperchromicity to a dye to phosphate ratio (D/P) that is equal to 0 (not shown), the molar extinction coefficient of the bound dye ($E_{474,B}$) was calculated at 474 nm, i.e. at the isosbestic point for the AO monomer–dimer system (Table 1). The concentrations of the free (C_F) and bound (C_B) dye were calculated for each point of titration. The results were then presented on a Scatchard plot and, using the computer interactive program, compared with the theoretical isotherm according to the McGhee and von Hippel equation [8]:

$$\frac{r}{C_F} = K_I(1-n\cdot r)\left[\frac{1-n\cdot r}{1-(n-1)\cdot r}\right]^{n-1} \qquad (1)$$

where r = binding density ($r = 2C_B/C_{DNA}$; C_{DNA} is expressed in pmoles/l); K_I = intrinsic association constant (M^{-1}) of the non-cooperative binding; and n = binding site size (number of base pairs).

Using this approach, the association constant K_I was found to be $5 \times 10^4\,M^{-1}$. This value is considerably lower than the K_I of $2 \times 10^5\,M^{-1}$ found for aqueous solutions of dsDNA and AO [15]*, despite the fact that the latter constant was measured at higher ionic strength (0.15 M Na^+). The n value of 3 base pairs obtained in our experiment (Fig. 2) is within the limits of 2.5 to 3 base pairs reported for

* The authors of Ref. 15 used the affinity parameter σ which is in accordance with the intrinsic association constant K_I.

Table 1. Spectral and equilibrium data of acridine orange (AO) and its complexes with nucleic acids*

	Spectral data				Equilibrium data			
	λ_{max} (nm)	($E_{max}\cdot10^{-4}$ $M^{-1}cm^{-1}$)	Isosbestic point λ_i (nm)	$E_{474}\cdot10^{-4}$ $M^{-1}cm^{-1}$	$K_c\cdot10^{-5}$ M^{-1}	$K_i\cdot10^{-2}$ M^{-1}	$\omega\cdot10^{-7}$	n Nucleotides
Standard buffer + ethanol (25%, v/v); Nucleic acid–AO complexes								
poly(rA)	457	(4.76)	468	2.18	2.06	4.9	4.2	1
poly(rI)	458	(3.09)	458	1.54	1.39	6.8	2.0	1
poly (rC)	426	(1.62)	444	0.47	1.15	3.1	3.7	1
poly(rU)	438	(2.28)	450	0.80	0.36	0.32	11.2	1
Calf thymus DNA	504	(6.00)	502	3.17		500†	0.01	3‡
AO aggregation								
AO (monomer)	494	(7.67)	474	4.67		9.0§		
AO (dimer)	468	(~7)						
Aqueous standard buffer								
AO (monomer)	482‖	(6.58)‖	470‖			91.0§		
AO (dimer)	467‖	(6.37)§						

* Abbreviations: λ_{max}, absorption maximum; E, molar extinction coefficient at wavelength λ; K_c, K_i, ω, and n, cooperative and intrinsic association constants, cooperativity parameter, and binding site size as defined by McGhee and von Hippel [8].

† K_i.

‡ Base pairs.

§ Calculation according to Ref. 12.

‖ Data from Ref. 12.

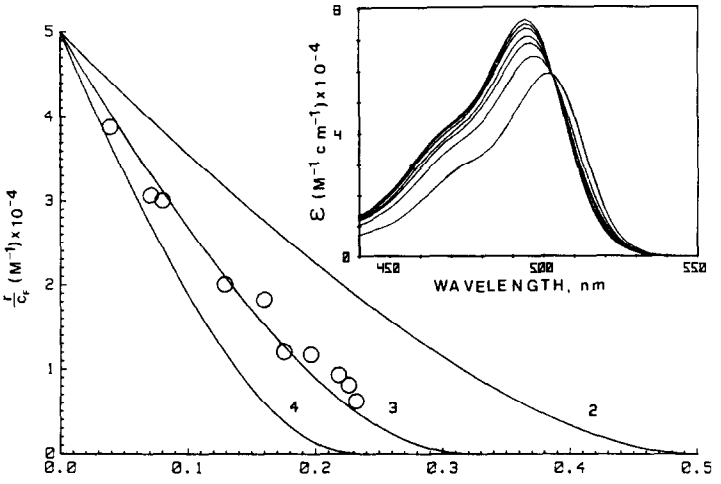

Fig. 2. Scatchard plot of the spectrophotometric titration (at 474 nm) of calf thymus DNA (52 μM) with AO [in standard buffer, 25% (v/v) ethanol] fitted to the McGhee–von Hippel probabilistic model [8]. Solid lines: the computer-drawn isotherms represented by equation 1 calculated for $n = 2$, 3 or 4 base pairs and $K_I = 5.0 \times 10^4\ M^{-1}$. Open circles: experimental points. Insert: The changes in molar extinction coefficient of AO during DNA titration. The upper curve represents the free dye; next curves from top to the bottom represent spectra of the mixtures of AO and DNA at D/P ratios of 0.95, 0.48, 0.19, 0.093, 0.031 and 0.003 respectively.

AO in aqueous solutions by various authors [e.g. Refs. 3, 4 and 7].

Figure 3 presents the spectra of mixtures of AO with poly(rA), poly(rC), poly(rI) and poly(rU) at several D/P ratios, in the presence of 25% ethanol. The spectra are characterized by the presence of distinct isosbestic points located at different wavelengths for each polymer. The inability to observe clear isosbestic points in earlier studies (e.g. Ref. 16) was most likely a consequence of the presence of AO dimers, eliminated here by the use of ethanol as a cosolvent. Another characteristic feature of the spectra is the distinct difference in their shapes, depending on the type of homopolymer.

The spectra of complexes of AO with different homopolymers (Fig. 4) were calculated under the assumptions that: (i) the amount of AO dimers was negligible (Fig. 1), and (ii) free AO contributes to at least 99% of the absorption at 494 nm [12]. The first assumption is based on the fact that, at low free dye concentration (~ 10 μM), the AO dimer concentration was below 2% in 25% ethanol. The second assumption [12] seems to be valid in light of the observation that the Scatchard plots calculated from absorption (at 474 and 494 nm) and fluorescence emission (at 525 nm) provided the same data (Fig. 5C). The spectrum of the AO–dsDNA complex, obtained by extrapolation (D/P → 0) from the data of the titration experiment illustrated in Fig. 2, is also included (Fig. 4) for comparison. Some numerical data of these spectra are included in Table 1.

The Scatchard plots calculated from titration data of four homoribopolymers are shown in Fig. 5. The values of $E_{474.F}$ and $E_{474.B}$ (474 nm is the isosbestic point for the free AO monomer–dimer system) were used for the calculations (Table 1). The plots show characteristic "humps", typical of cooperative reactions [8]. The shapes clearly indicate, however, that at least two different processes occur, namely, a cooperative one followed by a second phase that appears to be non-cooperative, but which, we believe, is an artifact of the solute–solid phase transition [e.g. poly(rA)] (Fig. 5A).

Calculations of the parameters of the first process were based on the McGhee–von Hippel model assuming cooperativity of the reaction [8]. The following formula was used:

$$\frac{r}{C_F} = K_i(1 - n \cdot r) \left[\frac{(2\omega - 1)(1 - n \cdot r) + r - R}{2(\omega - 1)(1 - n \cdot r)}\right]^{n-1} \left[\frac{1 - (n+1) \cdot r + R}{2(1 - n \cdot r)}\right]^2 \quad (2)$$

where $R = \{[1 - (n+1) \cdot r]^2 + 4 \cdot \omega \cdot r(1 - n \cdot r)\}^{0.5}$. The intrinsic association constant K_i represents the binding of the ligand molecule to the isolated binding sites of the polymer. The cooperative association constant of the ligand binding in a singly contiguous fashion $K_c = K_i \cdot \omega$, where ω is the cooperativity parameter and n is the binding site size of the polymer expressed in nucleotide units [8].

The theoretical curves which best fit the experimental points (Fig. 5) were constructed using computer-interactive programs based on the strategy described by Wilson and Lopp [10]. In the calculations, the n values of 2 for purine- and of 1.4–1.5 for the pyrimidine-homopolymers were used. The values of n, K_i and ω are listed in the legend to Fig. 5.

The titration data also can be expressed as a change of the extinction coefficients (for one or more wavelengths) and compared with the theoretical titration curves which, in turn, were constructed based on the parameters n, K_i and ω obtained from the Scatchard plot (Fig. 6). The theoretical titration curves were drawn by the computer according to the equations:

$$V_i = r_i \cdot B\,[C_p^0 \cdot f(r_i) + 1]\,[C_{AO}^0 \cdot f(r_i) - r_i]^{-1} \quad (3)$$

$$E_{\lambda.i} = [(V_i \cdot C_{AO}^0 - B \cdot r_i \cdot C_p^0) \cdot E_{\lambda.F} + r_i \cdot B \cdot C_p^0 \cdot E_{\lambda.B}]\,(V_i \cdot C_{AO}^0)^{-1} \quad (4)$$

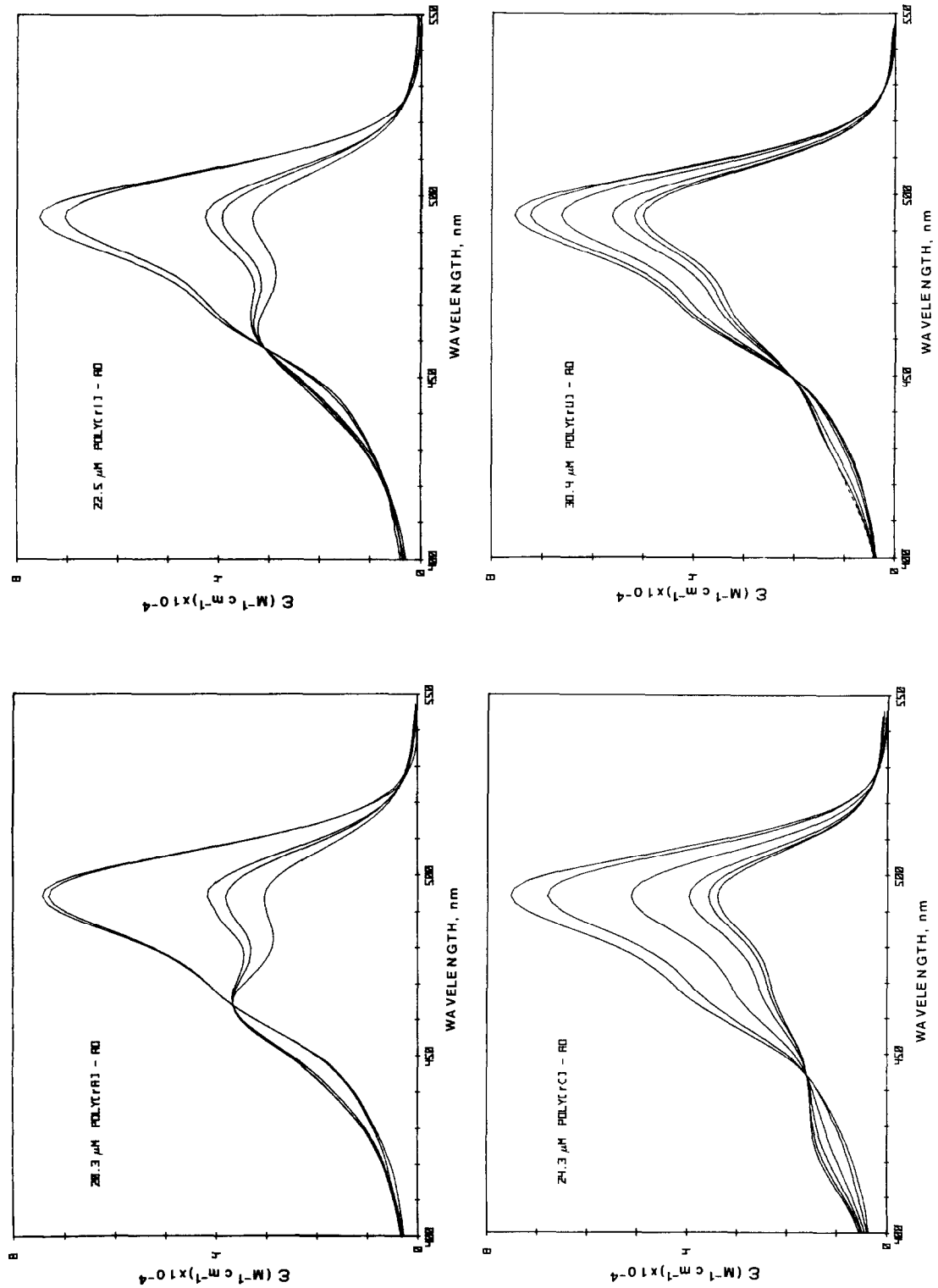

Fig. 3. Absorption spectra of AO in the presence of homoribopolymers [in standard buffer, 25% (v/v) ethanol] at various D/P ratios from 0 to 1.

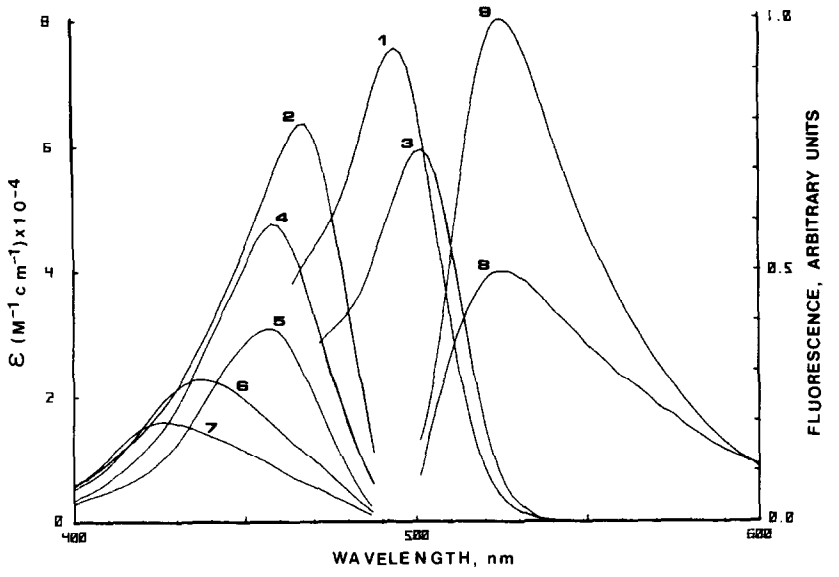

Fig. 4. Absorption spectra (left ordinate) of: (1) AO monomer; (2) AO dimer; (3) AO-dsDNA; (4) AO-poly(rA); (5) AO-poly(rI); (6) AO-poly(rU); and (7)AO-poly(rC). Fluorescence emission spectra (right ordinate) of: (8) AO monomer and; (9) AO-dsDNA. All spectra except spectrum 2 were recorded in standard buffer, 25% (v/v) ethanol. Spectrum 2 was measured in the absence of ethanol. Fluorescence spectra were not corrected for the emission monochromator and phototube responses. Spectra were calculated as described in the text, using data from experiments in Figs. 1–3.

where $f(r_i)$ is the value of the McGhee–von Hippel function (Eqn. 2) calculated for $0 < r_i < 1/n$ and $E_{\lambda,i}$ M^{-1} cm^{-1} is the extinction coefficient of the mixture of the V_i volume of stock AO solution at concentration C^0_{AO} and the B volume of the polymer at the initial concentration C^0_P (M, nucleotides)*.

The calculations can be done for any wavelength λ provided that the molecular extinction coefficients of free ($E_{\lambda,F}$) and bound ($E_{\lambda,B}$) ligand are known. Since deviations from the Beer–Lambert law are not taken into consideration in equations 3 and 4, the most accurate data are obtained using the wavelength of the isosbestic point of the AO monomer–dimer system. The above approach makes it possible to estimate directly the deviation of the experimental points from the theoretical titration curve. As can be seen from Fig. 6, the deviations were small for a large part of the experimental data. Despite that, the detailed analysis of the data, which will be given in detail later (Discussion), provides strong evidence that there is only one type of AO–ss-nucleic acid interaction, with binding site $n = 1$ nucleotide for all homopolymers, and the results of titrations, especially for $r > 0.4$, were strongly affected by a phase (solute–solid state) transition of the complex. Such a transition is evident from the data of the nephelometric titration of poly(rA) with AO (Fig. 7). Since the error of measurement is smaller for lower r values, $0.05 \leq r \leq 0.3$ was chosen arbitrarily for calculation of the set of parameters characterizing the homoribopolymer–AO interactions (Table 1, Fig. 8). The calculations were made using the method described above but with the assumption that $n = 1$ for all the polymers studied.

It should be noted that, although the value of the cooperative association constant ($K_c = K_i \cdot \omega$) was calculated with good accuracy and reproducibility [several repetitive experiments indicated a standard deviation of less than 10% (not shown)], accurate values of the intrinsic association constant, K_i, and the cooperativity coefficient, ω, were more difficult to obtain, and the standard deviation of the repeated measurements was higher (below 30%).

To better characterize the nature of the interactions, the effect of ethanol on AO binding was studied in more detail (Fig. 9). For poly(rA) and poly(rI) a linear relationship was observed between log K_i, log K_c and ethanol concentration, e.g.

$$\log K_i = A_0 + A_1 \cdot [\text{ethanol}] \qquad (5)$$

where A_0 represents the extrapolated value of log K_i at 0% ethanol concentration and A_1 is the slope (Fig. 9). The regression coefficients A_1 and A_0 are listed in Table 2.

The experiments show that the changes in the cooperative association constants, K_c, for both RNAs studied were due to changes in the intrinsic binding constants, because the cooperativity factors varied little with change in ethanol concentration. These data are not consistent with the classical stacking mechanism of dye binding [12, 17]; the effect of ethanol on cooperativity is expected to be much more pronounced than on K_i in a process involving dye–dye stacking.

Preliminary experiments indicated that AO shows

* Equations 3 and 4 were obtained by combining the equations:
$C_F + C_B = C^0_{AO} \cdot V/(B + V)$, $C_F = r/f(r)$ (from Eqn. 2), $C_B = r \cdot C^0_P \cdot B/(B + V)$, and $E_\lambda = (E_{\lambda,B} \cdot C_B + E_{\lambda,F} \cdot C_F)/(C_B + C_F)$.

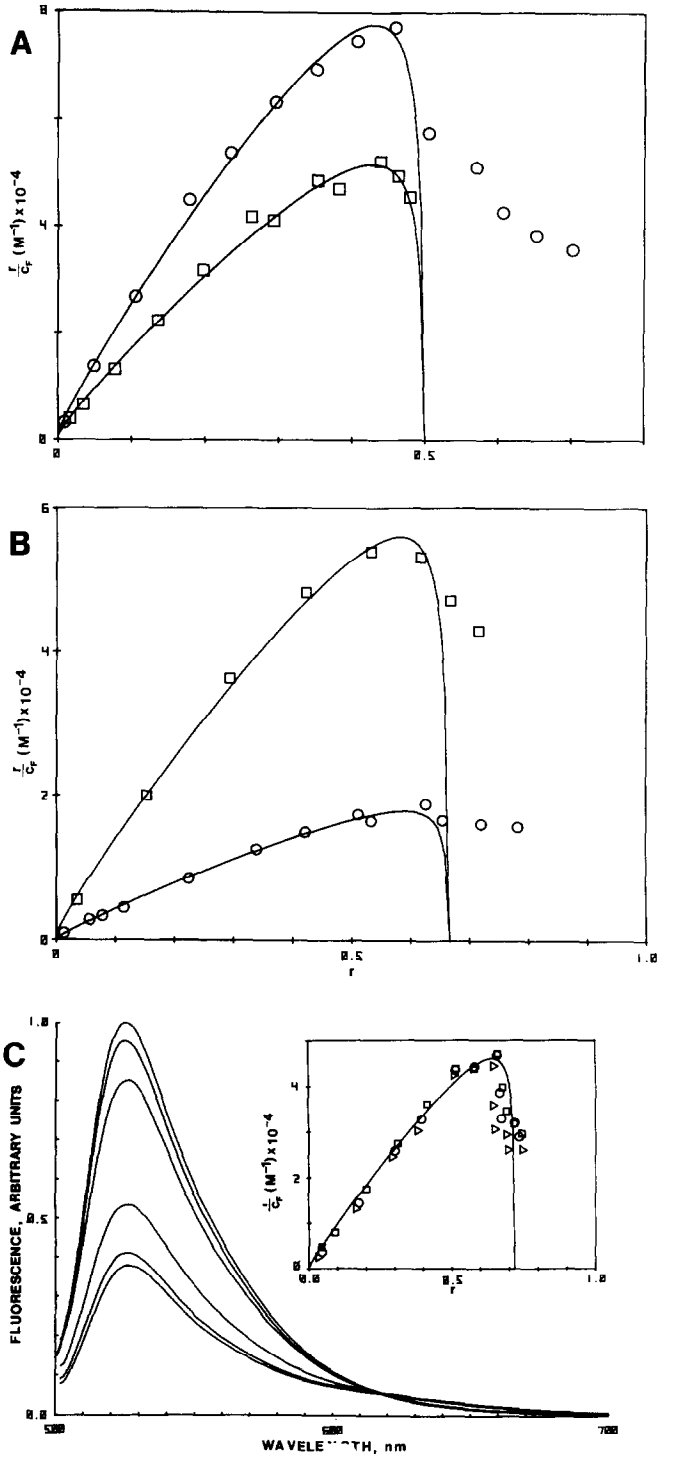

Fig. 5. Scatchard plots of the spectrophotometric titration of different homoribopolymers with AO [standard buffer, 25% (v/v) ethanol]. Solid line: the computer-drawn isotherms obtained based on equation 2, fitting the experimental points (-○-, -□-) with values of K_i, ω and n (given in parentheses).
(A) -○- poly(rA) (1000, 220, 2)(-□- poly(rI) (700, 210, 2).
B) -○- poly(rU) (130, 277, 1.5); -□- poly(rC) (560, 277, 1.5).
(C) Fluorimetric titration (excitation 474 nm) of poly(rC) (21.3 μM) with AO [standard buffer, 35% (v/v) ethanol]. D/P ratios from top to bottom: 0; 0.45; 0.68; 0.90; 1.35; 1.80. Insert: The Scatchard plot calculated from (-▷-) fluorescence measurement (with assumption that AO fluorescence at 525 nm is completely quenched when complexed with ss nucleic acids); or spectrophotometric measurement at 474 (-□-) and 494 nm (-○-). Solid line: the computer-drawn isotherm for $K_i = 300\ M^{-1}$, $\omega = 285$, $n = 1.39$ (nucleotides). The actual binding size $n = 1$; The corrected values of the other parameters are presented in Table 1.

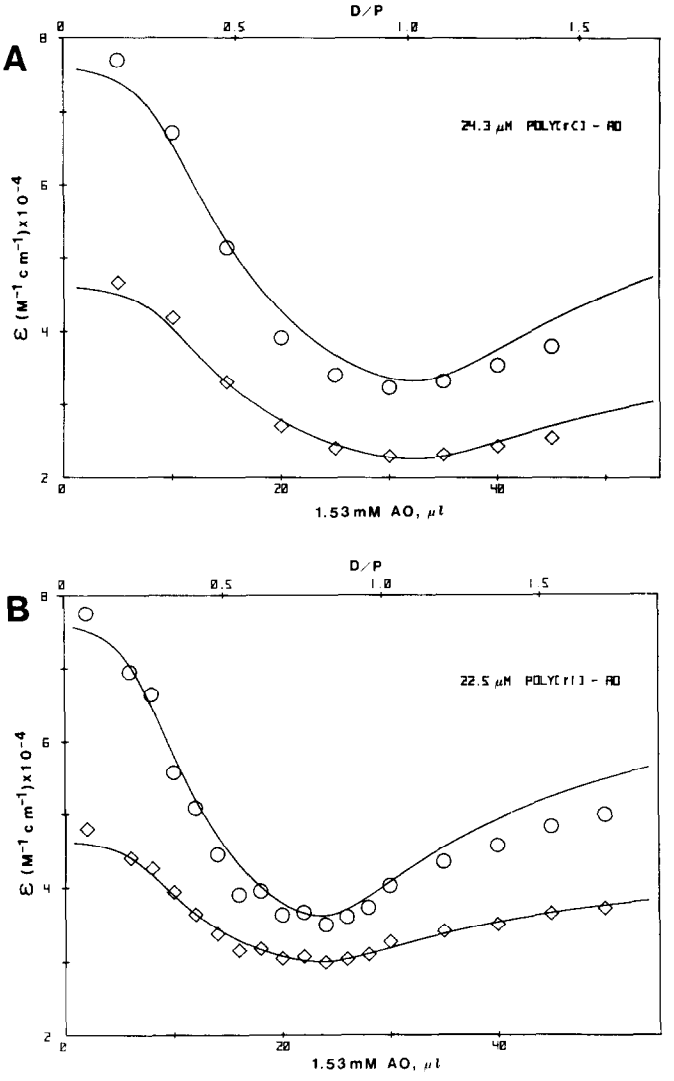

Fig. 6. Titration experimental points (symbols) and their fit-curves (solid lines), expressed as change of molecular extinction coefficient of AO (-○- at 494 and -◇- at 474 nm). The theoretical fit-curves were drawn by the computer after equations 3 and 4, using values of K_i, ω and n as listed in the legend to Fig. 5. (A) poly(rC); and (B) poly(rI).

Table 2. Effect of ethanol concentration on AO binding to ss RNA*

	Ethanol; mol % (X)				Regression coefficients		
	3.9	11.8	19.6	27.5	A_0	A_1	Standard error of estimation of A_0 on X
(a) poly(rA):							
log K_c	6.12	5.56	4.98	4.45	6.40	−0.071	0.015
log K_i	3.42	2.75	2.13	1.67	3.67	−0.075	0.076
log ω	2.70	2.81	2.85	2.78	2.73	+0.004	0.064
(b) poly(rI):							
log K_c	5.85	5.42	4.89	4.30	6.15	−0.066	0.056
log K_i	3.55	3.16	2.58	2.09	3.84	−0.063	0.055
log ω	2.30	2.27	2.30	2.22	2.32	−0.003	0.034

* Solvent: 10 mM Hepes, pH 7.0. Key: (a) 50 mM NaCl; (b) 25 mM NaCl. Binding parameters have been calculated as described in Results with the assumption that $n = 1$.

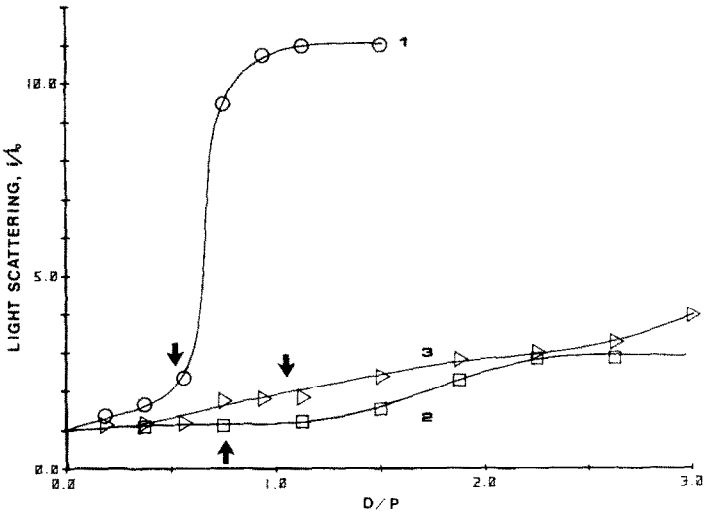

Fig. 7. Nephelometric titration of poly(rA) (concn = 21 μM) with AO in the absence (curve 1) and presence of ethanol (curve 2 - 25%; curve 3 - 35%, v/v). The intensity of the scattered light is expressed as a ratio of the intensity of the light dispersed by the sample "i" to the initial intensity of light dispersed by nucleic acid solution without AO, "i_0". The arrows indicate points of titration in which binding density $r = 0.5$.

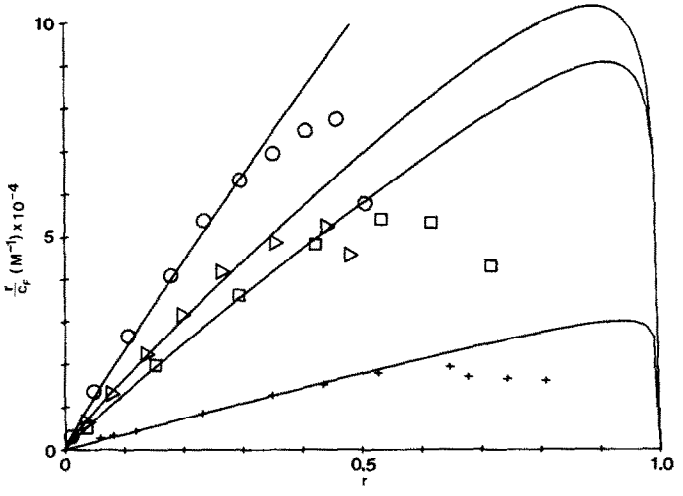

Fig. 8. Scatchard plot of the spectrophotometric titration of homoribopolymers: (○) poly(rA); (▷) poly(rI); (□) poly(rC) and (+) poly(rU). Solid lines represent the best fit of isotherms obtained (equation 2) at $0.05 \leq r \leq 0.3$, with the assumption that $n = 1$ (parameters K_i and ω are listed in Table 1).

significantly lower affinity towards deoxyribohomopolymers poly(dA), poly(dC), poly(dU) and poly(dT) than towards their respective ribo-analogs. Thus, the intrinsic association constant K_i was found to be 2.28×10^3 and 0.40×10^3 M^{-1} for poly(rA) and poly(dA) and the estimated cooperativity coefficient ω was 65 and 69 respectively (measured in 10 mM NaCl, 10 mM Hepes, 1 mM EDTA, 25% ethanol, pH 7.0). While deoxyribopolymers (C_p^0 = 30 μM, the same buffer) did not show a tendency toward complex formation up to 50 μM AO, the cooperative transition of ribohomopolymers was already evident at 4–25 μM dye concentration (not shown).

DISCUSSION

Models describing AO binding to ss-nucleic acids. According to generally accepted views, binding of AO to ss-nucleic acids, especially at a high D/P ratio, involves the formation of dye stacks ("dye stacking") along the nucleic acid backbone (for reviews, see Refs. 3, 4 and 17). As summarized recently by von Tscharner and Schwarz [12], three consecutive steps can be distinguished in the course of the binding process. During the first step (nucleation), the dye attaches electrostatically to the phosphates of the polyanion. The second step involves dye rotation around the nucleic acid backbone and its transient

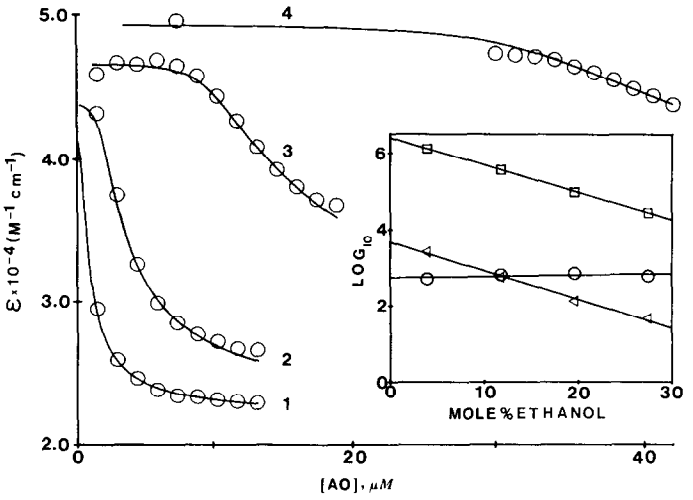

Fig. 9. Titration of poly(rA) with AO at different ethanol concentrations. Curves 1 to 4 represent 3.9, 11.8, 19.6 and 27.5 mol % of ethanol, respectively, in 50 mM Na^+, 10 mM Hepes, pH 7.0. The experimental points (-○-) are compared with the theoretical curves (solid lines), which are drawn by computer-based equations 3 and 4, using the equilibrium data listed in Table 2. The corrections for the ethanol concentration dependence of the extinction coefficient of free dye have been made (Fig. 1). The polymer concentrations were: 22.6, 24.2, 20.9 and 45.2 μM from curves 1 to 4 respectively. Insert: The regression of equilibrium constants according to equation 5: (□) log K_c, (△) log K_i and (○) log ω, as a function of cosolvent concentration.

intercalation between neighboring bases. With a further increase in D/P ratios, the third step, dye–dye stacking, is believed to occur. In this step AO molecules rotate back to the side of the polymer opposite to bases and form long stacks which are attached electrostatically to the phosphates [12].

The possibility of such intercalation during AO binding has been suggested in numerous studies [3, 18, 19] and the terms "partial" or "sandwich" intercalation were proposed to discriminate this type of binding from the intercalation into double helical molecules [12]. The intercalative structure of poly(rA)–AO complexes is also strongly supported by recent findings in which the induced circular dichroism of the dye was observed [20]. In studies on binding of proflavine (3, 6-diaminoacridine) to ss-nucleic acids, to explain optical properties of the complexes, Dourlent and Helene [5] suggest that the dye may be partially intercalated also during the final step of binding. According to our observations [6], a similar mechanism may also explain spectral properties of AO–ssRNA complexes.

The model proposed by us recently postulates partial intercalation of AO between the adjacent bases, resulting in the formation of dye-base alternating costacks of a strongly hydrophobic nature. A collapse of the polymer structure (precipitation of the complex), which in time is associated with changes of spectral properties, is a consequence of such interactions [6]. In contrast to previous models [12, 20], our model assumes that partial intercalation (dye–base costacking) is present throughout the whole range of binding density [6]. Arguments in support of this model are provided below.

Effects of ethanol on AO and nucleic acids. In the earlier experiments, because of poor solubility of the product, studies on interactions of the dye with nucleic acid, especially at higher D/P ratios, were severely limited. Introducing ethanol into the reaction mixture in the present experiments helped us to circumvent this problem. The question, therefore, may be raised as to what extent the results obtained in its presence may be extrapolated to aqueous media. To answer this question, the effects of ethanol on the substrates and on the reaction itself were studied in separate experiments.

With respect to AO, ethanol diminished dimerization, stacking or intercalation of the dye monomer. This effect was concentration dependent and could be extrapolated to zero concentration (Figs. 1 and 9, Table 2). Initially, the traditional hydrophobic interactions (and thus a strong requirement for water) were implicated in dye dimerization or stacking. Recent studies, however, provide evidence that the bulk solvent properties do not correlate with the kinetics of association of dyes similar to AO. The solvation model, therefore, was proposed in which the stacking forces of the dye are determined by specific dye–solvent interactions [21, 22]. According to the model, dye stacking in the presence of ethanol is decreased because relatively strong solvation complexes (AO–ethanol) are formed. This solvation process competes, in a sense, with any reaction in which a dye is involved, i.e. polymerization, stacking or intercalation. Our present data conform with the solvation model.

Ethanol, like most organic solvents, destabilizes the double helix. At lower concentrations, however, the effects are modest. Recent studies by Albergo and Turner [23] show that ethanol, at concentrations up to 27% (v/v), does not change significantly the thermodynamic properties of the double helix. Only at higher concentrations (> 50%, v/v) does it affect DNA conformation, presumably by inducing a transition from the B to C form. The effect of ethanol on ds-nucleic acid was also explained recently in light of the solvation mechanism rather than by traditional hydrophobic interactions. Thus, the changes in the

bulk solvent have a minor effect (mostly entropic) on the double helix until it begins to be dehydrated. It appears, therefore, that hydrophobic interactions are much less affected by the solvent than was initially thought [23].

Some ss-homoribopolymers have well developed secondary structures in solution. At pH 7.0, poly(rA) and poly(rC) are believed to have helical structures, while poly(rU) or poly(rI) have a random-coil conformation over a wide range of salt concentrations [24–28]. Both electronic and solvent forces appear to play a role in the bases' stacking interactions which dominate the thermodynamics of the helix formation [29–31]. Generally, the effect of ethanol on the stability of the helical structure of ss-homoribopolymers was similar to that observed for ds-structures. Destabilization of the helical conformation was evidenced by a marked decrease in the equilibrium constant for the random coil-helix poly(rA) transition. In analyzing this effect, however, one has to take into account that changes in the extinction coefficient are also attributed to dissociation of solvent molecules bound by hydrogen bonds to the bases, both in the helical and coil forms [31]. The melting profiles and laser temperature jump study of poly(rA) and poly(rC) indicate that they still have some helical arrangement in 27% (v/v) ethanol [29–31]. Thus, interactions in the presence of ethanol are not qualitatively different from those occurring in an aqueous environment, and the effects of ethanol, which are concentration dependent, may be extrapolated to zero concentration of this cosolvent (Fig. 9 and Table 2).

Structure of the complex. Ethanol simplified our studies of AO–nucleic acid interacions by drastically reducing dye aggregation (Fig. 1) and suppressing cooperative agglomeration of the complex (Fig. 7). As a consequence, distinctive isosbestic points, never clearly seen before, could be observed for all polymers studied (Fig. 3).

The presence of isosbestic points over a wide range of D/P at first sight appears to be inconsistent with the cooperative mode of dye–polymer interactions or implies that the dye molecules, bound with 0, 1 or 2 neighbors, all have the same absorption spectra. This inconsistency, however, is more apparent than real. Namely, according to the theory of ligand–polymer interaction [8], the ratios of probabilities of finding bound ligand molecules with 0, 1 or 2 nearest neighbors are equal to $K_i:K_i\cdot\omega:K_i\cdot\omega^2 = \omega^{-2}:\omega^{-1}:1$ respectively. Under the assumption that $\omega = 100$ (which is conservative), the respective ratios are $10^{-4}:10^{-2}:1$. Thus, the long dye clusters prevail even at moderately low D/P, and more than 99% of the bound dye molecules have two adjacent binding sites occupied by other molecules of the dye. The effects of 0 or 1 neighbor frequencies on the observed spectra are, therefore, negligible. Despite this fact, however, the titration patterns still were not entirely clear (Fig. 5). Specifically, the Scatchard plots indicated two phases of the reaction: while the first phase indicated the cooperative interactions, the second phase was initially difficult to interpret.

Careful analysis of these data, as well as other observations [6], convinced us that the solute-solid state transition, occurring at higher binding density even in the presence of ethanol (Fig. 7), disturbed not only optical measurements but also the equilibrium of the reaction and was responsible for the second phase of the titration plots. Specifically:

(1) No clear explanation is provided by the stacking or partial intercalation models for the larger binding sites of purine compared with pyrimidine-homoribopolymers (2 vs 1.5 nucleotides) under the same conditions. The difference in solubility or ability to aggregate thus may be responsible for this discrepancy.

(2) The size of the binding site, n, calculated with an assumption of two types of interactions decreases with increasing ethanol concentration. The calculation for poly(rA) in 0, 25 and 35% ethanol showed $n = 2.5$, 2 and 1.4 nucleotides respectively (not shown).

(3) The nephelometric measurements indicated formation of large (>0.35 μm) particles during titration of poly(rA) (Fig. 7. [6]). This is direct evidence of the solute-solid state transition, occurring at $r > 0.5$, which may be mistakenly considered as cooperative dye–dye stack formation [12].

Considering the above, the assumption was made that $n = 1$ (see also evidence provided before [6], and this value was used for further calculations. It should be emphasized that, because the net slope of the cooperative isotherm equals $K_i(2\omega\text{-}2n\text{-}1)$ [8], the results of calculations, as proposed, are less dependent on n when $n << \omega$.

Several present findings cannot be explained by the stacking model and its modifications [12, 17, 20] of AO–nucleic acid interactions. Namely:

(1) The presence of well defined isosbestic points during titration (Fig. 3) indicates that only one type of product existed throughout the whole range of D/P ratios. Thus, no evidence can be found that AO rotates around the backbone of nucleic acids and, depending on the D/P ratio, at first forms intercalative and then dye–dye stacking structures [12].

(2) The Scatchard plots (Figs. 5 and 8) clearly indicate that the reaction was cooperative from the onset of titration. According to the stacking model, cooperativity is expected to be manifested only at higher D/P ratios, while the initial binding should be noncooperative [12].

(3) There were significant differences in the absorption spectra of the complexes with different RNA types depending on the base composition (Fig. 4). These differences, noted before by others, were explained either as due to a different orientation between adjacent dye molecules in the stack bound to different lattices or as a result of different degrees of dye aggregation [17, 32, 33]. The first explanation, however, contradicts the observation that spectral properties of the complexes are related to base composition (purine vs pyrimidine) rather than to the secondary structure of the polymers (Fig. 4, [6, 34]). The second explanation fails in light of the well defined isosbestic points in the AO–ssRNA system (Fig. 3), which is not consistent with a mixture of AO-stacks of varying length. At a given n and ω, the average cluster length is related to the binding density r, which varies [8].

(4) When the absorption maxima bands of the AO–RNA complexes (calculated for low binding

density $r < 0.5$) are compared with the emission maxima of the solid, saturated ($r = 1$) complexes [6], mirror symmetry is evident (Fig. 10). Such symmetry is expected only if one type of binding characterizes both high and low binding density, and if the structure of the complex is determined by the base composition. If the spectral differences were related to different lattices of the polymer, the probability of such a correlation between the polymer in solution vs the precipitate would be negligible.

(5) Both the intrinsic (K_i) as well as the cooperative ($K_c = K_i \cdot \omega$) association constants correlate with the RNA-base composition (purines vs pyrimidines) but not with the secondary structure of the polymers. Two of the polymers investigated, poly(rA) and poly(rC), have well defined helical structures; the other two are random coil structures in the salt concentration and pH range currently used [24–28].

(6) According to the stacking model, the dye–dye stack formation is the main force of cooperativity. Thus, one would expect that with the increase in ethanol concentration the cooperativity factor ω would be markedly lowered due to competitive dye–cosolvent interactions. On the other hand, if K_i represents the "nucleation" process [12], i.e. electrostatic attachment, its value should be little affected by ethanol; our data, however, indicate the opposite relationship [Figs. 1 and 9-insert; see poly(rA) and poly(rI), Table 2]. Thus, the data contradict the presence of dye–dye interactions as visualized in the classic model of dye stacking on the backbone of the nucleic acids. Further studies, however, are required (now in progress) to explain the relationship between changes of K_i and ω vs ethanol concentration according to the alternative models of AO–ss-nucleic acid complexes.

(7) According to the classical model, neither K_i nor ω is expected to correlate with base composition (purines vs pyrimidines). The equilibrium data (Table 1) showed high selectivity of AO binding with regard to base composition of the homoribopolymers*.

In summary, all the observations listed above cannot support the classic stacking model of AO interactions with ssRNA. On the other hand, these observations (especially the presence of well defined isosbestic points, high cooperativity from the onset of titration, differences in absorption, specific and equilibrium data in relation to different RNA types, and the mirror symmetry of the absorption vs emission spectra) all may be explained by our model [6] which we summarized in the first part of the Discussion.

Destabilizing effect of AO on the double helix. Free energy changes of the AO binding to ds- vs ss-nucleic acids (Table 3) bear interesting implications. Thus, as generally accepted, intercalation of the dye, which is characterized by the high association constant, increases the stability of the double helix [35]. This binding may be described as:

$$(Bp)_n + \mathrm{AO} \overset{K_I}{\rightleftharpoons} \mathrm{AO}_i(Bp)_n; \quad \Delta G_I^0 \qquad (6)$$

where Bp represents two nucleotides involved in base pairing, n is the binding site size for the intercalation ($n = 2$ or 3 [7]), and K_I is the association

* High cooperativity of the process makes it difficult, if not impossible, to observe this selectivity for natural polymers.

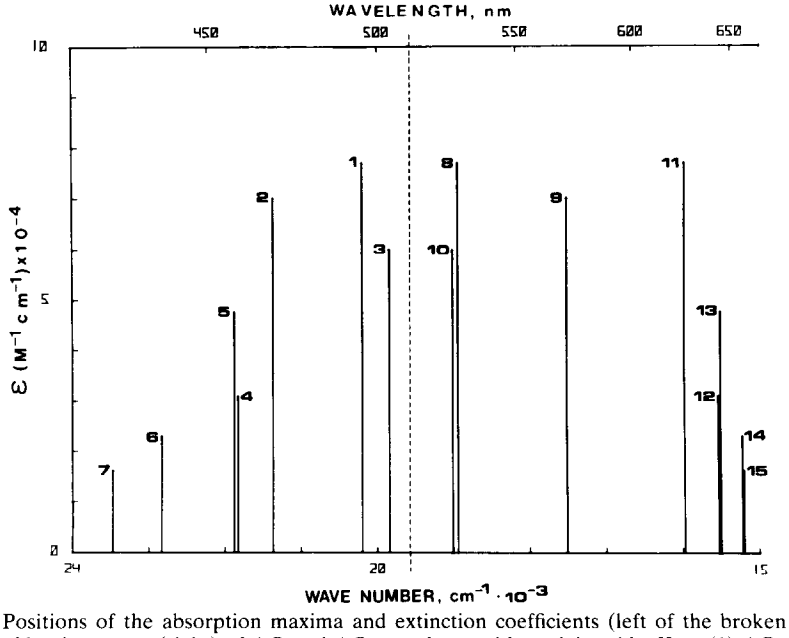

Fig. 10. Positions of the absorption maxima and extinction coefficients (left of the broken line) and maxima of luminescence (right) of AO and AO complexes with nucleic acids. Key: (1) AO monomer; (2) AO dimer; (3) AO-intercalated into dsDNA; (4) poly(rI)-AO; (5) poly(rA)-AO; (6) poly(rU)-AO; (7) poly(rC)-AO; (8) AO monomer; (9) AO dimer; (10) AO-intercalated into dsDNA; (11) AO aggregates (crystals) [6]; (12) poly(rI)-AO; (13) poly(rA)-AO; (14) poly(rU)-AO and (15) poly(rC)-AO. From 1 to 10 were all measured in standard buffer, 25% (v/v) ethanol; 12–15 were measured in buffer in the absence of ethanol (data from Ref. 6). While heights of the bars representing absorption are proportional to the respective E values (ordinate), weights of the luminescence bars are not scaled to be in proportion to fluorescence intensity or quantum yield.

Table 3. Standard free energy changes of the cooperative (ΔG_c^0) and non-cooperative (ΔG_i^0) interactions of nucleic acid with AO calculated per 1 mole of the dye (based on data from Table 1)

Polymer	kcal/mole $-\Delta G_c^0$	$-\Delta G_i^0$
poly(rA)	7.25	3.67
poly(rI)	7.02	3.86
poly(rC)	6.90	3.40
poly(rU)	6.21	2.05
ds DNA		6.41

constant of this binding; AO_i indicates that the dye molecule is bound by intercalation.

Additionally, AO can be attached via electrostatic forces to the remaining $(2n-1)$ phosphate groups (i.e. to the phosphates not neutralized by the already intercalated AO cation), outside of the double helix [34]:

$$AO_i(Bp)_n + (2n-1)AO \overset{KE}{\rightleftharpoons} AO_i(Bp)_n AO_{E(2n-1)}; \quad \Delta G_E^0 \qquad (7)$$

where AO_E represents the dye bound by the "weak" interactions (external to the double helix) and K_E is the association constant of this binding. The cooperativity in the dye–dye interactions (stacking) outside the double helix is rather low ($\omega = 1.25$) [36]. Because $K_I >> K_E$ (at moderate and high ionic strength), at low D/P most AO will bind preferentially by intercalation. After saturation of the intercalation sites, the dye will bind externally to ds- or ss-regions. Considering the dynamic structure of nucleic acids, the ss-regions become available during "breathing" of the double helix [37, 38]. Because binding of AO to ss-regions is highly cooperative ($\omega > 10^2$; Table 1), the binding will expand inducing denaturation of the adjacent ds-regions. This reaction can be described as:

$$AO_i(Bp)_n + (2n-1)AO \overset{K}{\rightleftharpoons} 2nAO{\cdot}B; \qquad \Delta G^0 \qquad (8)$$

where base pairing (Bp) is broken and AO binding can now be related per individual nucleotide (base; B). The above process is competitive with the external binding to the ds helix (Eqn. 7) and requires dissociation of the intercalative complex (Eqn. 6), and denaturation of the double helix. The approximate free energy change ΔG^0 of the process described by Eqn. 8 can, therefore, be calculated (e.g. for RNA) according to:

$$\Delta G^0 = \Delta G_c^0 - \Delta G_I^0 - \Delta G_E^0 - \Delta G_D^0 = -2.7 \text{ kcal/mole (per nucleotide)} \qquad (9)$$

where $\Delta G_c^0 = -6.9$ cal/mole (per 1 nucleotide, average for cooperative AO complex formation, established based on studies of four different ss-homopolymers, Table 3); $\Delta G_I^0 = -1.6$ kcal/mole, free energy change of the intercalative AO binding into the double helix (Eqn. 6) calculated per 1 nucleotide, with the conservative assumption that $n = 2$ (base pairs) (Table 3); and $\Delta G_E^0 = -1.2$ kcal/mole. Free energy change of the external AO binding to ds-helix may be considered as $\Delta G_E^0 = \Delta G_{el}^0 + \Delta G_{st}^0$, where ΔG_{el}^0 represents electrostatic binding of AO to the ds helix [39]. Although ΔG_{el}^0 was not established for AO, its value is probably close to the one describing binding of charged amino groups of lysine to poly(rA)·poly(rU) where ΔG_{el}^0 has been found to be -1.15 kcal/mole (in 0.1 M NaCl, at pH 7.0, 4°) [11]. The ΔG_{st}^0 component represents stacking of AO molecules outside the double helix [39]. According to Stone and Bradley [36], this value is -0.07 kcal/mole.

The obtained value of ΔG_E^0 (-1.2 kcal/mole) is in agreement with the theoretical value calculated for proflavine by Gersch and Jordan [39]*. $\Delta G_D^0 = -1.4$ kcal/mole is the average free energy change for base pairing (per nucleotide) [44]. The extreme values are -0.6 kcal/mole (for A-U at the particular base pair configuration) and -2.4 kcal/mole (for G-C) [44].

The calculations (Eqn. 9) were made assuming that the intercalation of AO into dsRNA has similar free energy change as to dsDNA and that base pairing of RNA is continuous along the molecule; both assumptions are conservative. The calculation indicated that, even for the continuous G-C sequences of RNA (i.e. the lowest limit of ΔG_D^0), the value of ΔG^0 is -1.7 kcal/mole (per nucleotide).

The highly favorable free energy change of the denaturation process of RNA (Eqn. 8 and 9), as evident, is not only a result of the differences in AO association constants with ss- vs ds-regions, but also due to the different stoichiometry of the complexes, because ss-regions bind at least 4-fold more AO than can be intercalated into the double helix.

Because AO has lower affinity for ss-deoxyribo- than ss-ribopolymers [e.g. for poly(dA) $\Delta G_c^0 = -6.07$ kcal/mole as compared with $\Delta G_c^0 = -7.05$ kcal/mole for poly(rA); in 10 mM Na^+, 25% (v/v) ethanol, pH 7.0], it is expected that the destabilization of the secondary structure of DNA could also occur but will require higher concentration of the dye.

The described phenomenon may explain some earlier observations which appeared to contradict the stabilizing effect of intercalators on the double helix. Specifically:

(1) It was observed that AO prevented DNA renaturation [7, 45].

(2) The principle of differential staining of ds- vs ss-nucleic acids was used in cytochemistry to assay DNA vs RNA respectively, [46–48], despite the evidence that a large portion of cellular RNA (rRNA, tRNA and HnRNA) has a double stranded conformation. It was suggested, therefore, that AO *per se* could selectively denature dsRNA [46].

(3) The selectivity of DNA vs RNA assay disappears when the AO concentration reaches 5×10^{-5}

* The lower value obtained experimentally [40] seems to be too low to be accepted in a view of ion condensation theory of polyelectrolytes [11, 41, 42]. Therefore, most likely, two kinds of binding (Eqn. 7 and 8) contributed to these results [40]. Furthermore, at the ionic strength and AO concentration used by the authors [40], only red luminescence, characteristic of AO interactions with ss-nucleic acids, could be seen [43].

M (0.15 M Na^+, 24°, pH 7.4); above that concentration only the red luminescence, which is characteristic for ss-nucleic acids, can be seen [49].

(4) Using AO as a conformational probe for nucleic acids, Furano *et al.* [50] could not observe double helicity of rRNA *in situ*. Failure to detect ds-regions of rRNA, most likely, is a result of the denaturing effect of AO on RNA.

More direct evidence of the denaturing properties of AO was obtained recently when increased accessibility of the DNA (calf thymus) bases to two different conformational probes, formaldehyde and diethyl pyrocarbonate, was observed during formation or dissociation of the AO–DNA (1:1) complexes.*

The mathematical model for helix-coil transition of nucleic acids in the presence of ligands which bind to both ss- and ds-nucleic acids was developed by McGhee [35] and, according to the model, small ligands such as AO are expected to be especially effective in lowering the temperature of thermal transition. Our results strongly support this model.

Conclusions. Using ethanol as cosolvent in studies of AO–ss-nucleic acid interactions, several long standing problems (AO dimerization, precipitation of the complex) could be bypassed. The results of spectrophotometric and equilibrium studies support the dye–base costacking structure of the complex rather than dye–dye stacking visualized in the classic model.

The thermodynamics of the AO binding to ss- and ds-nucleic acids indicates that at high D/P ratios the double helix can be destabilized. Because binding of other intercalators (dyes, antitumor agents) may induce a similar denaturing effect (e.g. Refs. 5, 9 and 51), the observed phenomenon may be representative of more general processes such as those operating during the unfolding of DNA in chromatin for transcription or the transition of DNA from B to Z conformation (for review see Ref. 52) triggered by the regulatory molecules [35, 53, 54].

Acknowledgements—We wish to thank Dr. Thomas Sharpless for many stimulating discussions, Mr. Jay Ladenheim for technical assistance, and Dr. Frank Traganos and Ms. Robin Nager for their assistance in the preparation of the manuscript. This work was supported by United States Public Health Service Grants CA-28704, CA-232-96 and CA-14134 and was presented in part at the Eighth Conference on Analytical Cytology and Cytometry, Wentworth-by-the-Sea, New Hampshire, May 19–25, 1981. [Abstract: *Cytometry* **2**, 107 (1981).]

REFERENCES

1. M. J. Waring, *A. Rev. Biochem.* **50**, 159 (1981).
2. H. Porumb, *Prog. Biophys. molec. Biol.* **34**, 175 (1978).
3. A. R. Peacocke, in *Acridines* (Ed. R. M. Acheson), p. 723. Interscience, New York (1973).
4. Z. Darzynkiewicz, in *Flow Cytometry and Sorting* (Eds. M. R. Melamed, P. F. Mullaney and M. A. Mendelsohn), p. 359. John Wiley, New York (1979).
5. M. Dourlent and C. Helene, *Eur. J. Biochem.* **23**, 86 (1971).
6. J. Kapuscinski, Z. Darzynkiewicz and M. R. Melamed, *Cytometry* **2**, 201 (1982).
7. S. Ichimura, M. Zama, H. Fujita and T. Ito, *Biochim. biophys. Acta* **190**, 116 (1969).
8. J. D. McGhee and P. H. von Hippel, *J. molec. Biol.* **86**, 469 (1974).
9. J. Kapuscinski and W. Szer, *Nucleic Acids Res.* **6**, 3519 (1979).
10. W. D. Wilson and I. G. Lopp, *Biopolymers* **18**, 3025 (1979).
11. M. T. Record Jr., T. M. Lohman and P. DeHaseth, *J. molec. Biol.* **107**, 145 (1976).
12. V. von Tscharner and G. Schwarz, *Biophys. Struct. Mechanism* **5**, 75 (1979).
13. C. A. Parker, *Photoluminescence of Solutions*, p. 220. Elsevier, Amsterdam (1968).
14. G. Weill and M. Calvin, *Biopolymers* **1**, 401 (1963).
15. W. Muller and D. M. Crothers, *Eur. J. Biochem.* **54**, 267 (1975).
16. S. Yamabe, *Molec. Pharmac.* **3**, 556 (1967).
17. D. F. Bradley, *Trans. N.Y. Acad. Sci.* (2) **24**, 64 (1961).
18. D. S. Drummond, V. F. W. Simpson-Gildemeister and A. R. Peacocke, *Biopolymers* **3**, 135 (1965).
19. N. J. Pritchard, A. Blake and A. R. Peacocke, *Nature, Lond.* **212**, 1360 (1966).
20. T. Imae, S. Hayashi and S. Ikeda, *Int. J. biol. Macromol.* **3**, 259 (1981).
21. T. G. Dewey, P. S. Wilson and D. H. Turner, *J. Am. chem. Soc.* **100**, 4550 (1978).
22. T. G. Dewey, D. A. Raymond and D. H. Turner, *J. Am. chem. Soc.* **101**, 5822 (1979).
23. D. DePrisco Albergo and D. H. Turner, *Biochemistry* **20**, 1413 (1981).
24. D. N. Holcomb and I. Tinoco, *Biopolymers* **3**, 121 (1965).
25. G. D. Fasman, C. Lindblow and L. Grossman, *Biochemistry* **3**, 1015 (1964).
26. W. Szer, *J. molec. Biol.* **16**, 585 (1966).
27. S. B. Zimmerman, *J. molec. Biol.* **101**, 563 (1976).
28. C. H. Chou, G. J. Thomas, Jr., S. Arnott and P. J. Campbell Smith, *Nucleic Acids Res.* **4**, 2407 (1977).
29. T. G. Dewey and D. H. Turner, *Biochemistry* **18**, 5757 (1979).
30. T. G. Dewey and D. H. Turner, *Biochemistry* **19**, 1681 (1980).
31. S. M. Freier, K. O. Hill, T. G. Dewey, L. A. Marky, K. J. Breslauer and D. H. Turner, *Biochemistry* **20**, 1419 (1981).
32. R. Rigler Jr., *Acta physiol. scand.* **67** (Suppl. 267), 7 (1966).
33. S. Ichimura, *Biopolymers* **14**, 1033 (1975).
34. A. R. Peacocke and J. N. H. Skerrett, *Trans. Faraday Soc.* **52**, 261 (1956).
35. J. D. McGhee, *Biopolymers* **15**, 1345 (1976).
36. A. L. Stone and D. F. Bradley, *J. Am. chem. Soc.* **83**, 3627 (1961).
37. H. M. Sobell, B. S. Reddy, K. K. Bhandary, S. C. Jain, T. D. Sakore and T. P. Seshadri, *Cold Spring Harbor Symp. Quant. Biol.* **42**, 87 (1977).
38. R. S. Preisler, C. Madal, S. W. Englander, N. R. Kallenbach, F. B. Howard, J. Frazier and H. T. Miles, in *Biomolecular Stereodynamics* (Ed. R. H. Sarma), Vol. 1, p. 405. Adenine Press, New York (1981).
39. N. F. Gersch and D. O. Jordan, *J. molec. Biol.* **13**, 138 (1965).
40. R. W. Armstrong, T. Kurucsev and U. P. Strauss, *J. Am. chem. Soc.* **92**, 3174 (1970).
41. G. S. Manning, *Q. Rev. Biophys.* **11**, 179 (1978).
42. M. T. Record Jr., S. J. Mazur, P. Melancon, J-H. Roe, S. L. Shaner and L. Unger, *A. Rev. Biochem.* **50**, 997 (1981).

* J. Kapuscinski, Z. Darzynkiewicz and M. R. Melamed, *Combined International Conference on Analytical Cytology*. Schloss Elmau, F.R.G., October 17, 1982, Abstracts, p. 108.

43. F. Traganos, Z. Darzynkiewicz, T. Sharpless and M. R. Melamed, *J. Histochem. Cytochem.* **24**, 40 (1976).
44. P. N. Borer, B. Dengler and I. Tinoco Jr., *J. molec. Biol.* **86**, 843 (1974).
45. Z. Darzynkiewicz, F. Traganos, T. Sharpless and M. R. Melamed, *Biochem. biophys. Res. Commun.* **59**, 392 (1974).
46. Z. Darzynkiewicz, F. Traganos, T. Sharpless and M. R. Melamed, *Expl. Cell Res.* **95**, 143 (1975).
47. K. D. Bauer and L. A. Dethlefsen, *J. Histochem. Cytochem.* **28**, 493 (1980).
48. Z. Darzynkiewicz, F. Traganos and M. R. Melamed, *Cytometry* **1**, 98 (1980).
49. Z. Darzynkiewicz, F. Traganos, T. Sharpless, C. Friend and M. R. Melamed, *Expl. Cell Res.* **99**, 301 (1976).
50. A. V. Furano, D. F. Bradley and A. G. Childers, *Biochemistry* **5**, 3044 (1966).
51. J. Kapuscinski, Z. Darzynkiewicz, F. Traganos and M. R. Melamed, *Biochem. Pharmac.* **30**, 231 (1981).
52. A. Rich, G. J. Quigley and A. H-J. Wang, in *Biomolecular Stereodynamics* (Ed. R. H. Sarma), Vol. 1, p. 35. Adenine Press, New York (1981).
53. R. C. Kelly, D. E. Jensen and P. H. von Hippel, *J. biol. Chem.* **251**, 7240 (1976).
54. J-J. Toulme and C. Helene, *J. biol. Chem.* **252**, 244 (1977).